Inorg. Chem. **2005**, *44*, 4941–4946

Density Functional Study on Dihydrogen Activation at the H Cluster in Fe-Only Hydrogenases

Taijin Zhou,*,† Yirong Mo,*,‡ Zhaohui Zhou,† and Khirui Tsai†

Department of Chemistry, State Key Laboratory for Physical Chemistry of Solid States, Xiamen University, Xiamen, Fujian 361005, P. R. China, and the Department of Chemistry, Western Michigan University, Kalamazoo, Michigan 49008

Received November 2, 2004

Models simulating the catalytic diiron subcluster $[FeFe]_H$ in Fe-only hydrogenases have often been designed for computational exploration of the catalytic mechanism of the formation and cleavage of dihydrogen. In this work, we extended the above models by explicitly considering the electron reservoir $[4Fe\text{-}4S]_H$ which is linked to the diiron subcluster to form a whole H cluster ($[6Fe\text{-}6S] = [4Fe\text{-}4S]_H + [FeFe]_H$). Large-scale density functional theory (DFT) computations on the complete H cluster, together with simplified models in which the $[4Fe\text{-}4S]_H$ subcluster is not directly involved in the reaction processes, have been performed to probe hydrogen activation on the Fe-only hydrogenases. A new intermediate state containing an $Fe_p\cdots H\cdots CN$ two-electron three-center bond is identified as a key player in the H_2 formation/cleavage processes.

Introduction

Hydrogenases (or hereafter H_2ases) reversibly catalyze hydrogen oxidation ($H_2 \rightleftarrows 2H^+ + 2e^-$) and play a key role in hydrogen metabolism in many microorganisms, which use hydrogen as a source of electrons and protons or generate hydrogen as a way to reduce protons.[1−27] Recently, we systematically studied the mechanism of the enzymatic formation and cleavage of dihydrogen on the catalytic diiron subcluster, $[FeFe]_H$, of the H cluster in Fe-only H_2ases by simulating the active center, $[FeFe]_H$, with a simplified model, $\{[H](CH_3S)(CO)(CN^-)Fe_p(CO_b)(\mu\text{-}SRS)Fe_d(CO)(CN^-)L\}$, where [H] stands for the $[Fe_4S_4]_H^{2+}$ subcluster bridged to the $[FeFe]_H$ moiety and L can be any hydrogen species such as H^+, H^-, or H_2. On the basis of the above model, structures of various possible redox states were optimized and compared with the X-ray crystallographic structures and other accessible experimental evidence.[7,9,10,28−34]

* To whom correspondence should be addressed. Fax: +86-592-2183795. E-mail: tjzhou@xmu.edu.cn (T.Z.); ymo@wmich.edu (Y.M.).
† Xiamen University.
‡ Western Michigan University.

(1) Nicolet, Y.; Cavazza, C.; Fontecilla-Camps, J. C. *J. Inorg. Biochem.* **2002**, *91*, 1.
(2) Frey, M. *ChemBioChem* **2002**, *3*, 153.
(3) Cammack, R. *Nature* **1999**, *397*, 214.
(4) Evans, D. J.; Pickett, C. J. *Chem. Soc. Rev.* **2003**, *32*, 268.
(5) Rees, D. C.; Howard, J. B. *Science* **2003**, *300*, 929.
(6) Collman, J. P. *Nature Struct. Biol.* **1996**, *3*, 213.
(7) Nicolet, Y.; Piras, C.; Legrand, P.; Hatchikian, E. C.; Fontecilla-Camps, J. C. *Structure* **1999**, *7*, 13.
(8) Nicolet, Y.; Lemon, B. J.; Fontecilla-Camps, J. C.; Peters, J. W. *TIBS* **2000**, *25*, 138.
(9) Nicolet, Y.; de Lacey, A. L.; Vernede, X.; Fernandez, V. M.; Hatchikian, E. C.; Fontecilla-Camps, J. C. *J. Am. Chem. Soc.* **2001**, *123*, 1596.
(10) Peters, J. W.; Lanzilotta, W. N.; Lemon, B. J.; Seefeldt, L. C. *Science* **1998**, *282*, 1853 (Errata: 283, 35; 283, 2102).
(11) Peters, J. W. *Curr. Opin. Struct. Biol.* **1999**, *6*, 670.
(12) Holm, R. H.; Kennepohl, P.; Solomon, E. I. *Chem. Rev.* **1996**, *96*, 2239.
(13) Darensbourg, M. Y.; Lyon., E. J.; Smee, J. J. *Coord. Chem. Rev.* **2000**, *206*, 533.
(14) Darensbourg, M. Y.; Lyon, E. J.; Zhao, X.; Georgakaki, I. P. *Proc. Natl. Acad. Sci. U.S.A.* **2003**, *100*, 3683.
(15) Thauer, R. K.; Klein, A. R.; Hartmann, G. C. *Chem. Rev.* **1996**, *96*, 3031.
(16) Stein, M.; Lubitz, W. *J. Inorg. Biochem.* **2004**, *98*, 862.
(17) Niu, S.; Thomson, L. M.; Hall, M. B. *J. Am. Chem. Soc.* **1999**, *121*, 4000.
(18) Pavlov, M.; Siegbahn, P. E. M.; Blomberg, M. R. A.; Crabtree, R. H. *J. Am. Chem. Soc.* **1998**, *120*, 548.
(19) Cao, Z.; Hall, M. B. *J. Am. Chem. Soc.* **2001**, *123*, 3734.
(20) Fan, H.; Hall, M. B. *J. Am. Chem. Soc.* **2001**, *123*, 3828.
(21) Liu, Z. P.; Hu, P. *J. Am. Chem. Soc.* **2002**, *124*, 5175.
(22) Adams, M. W. W.; Stiefel, E. I. *Curr. Opin. Chem. Biol.* **2000**, *4*, 214.
(23) Pereira, A. S.; Tavares, P.; Moura, I.; Moura, J. G.; Huynh, B. H. *J. Am. Chem. Soc.* **2001**, *123*, 2771.
(24) Razavet, M.; Borg, S. J.; George, S. J.; Best, S. P.; Fairhurst, S. A.; Pickett, C. J. *Chem. Commun.* **2002**, 700.
(25) George, S. J.; Cui, Z.; Razavet, M.; Pickett, C. J. *Chem.—Eur. J.* **2002**, *8*, 4037.
(26) Dole, F.; Fournel, A.; Magro, V.; Hatchikian, E. C.; Bertrand, P.; Guigliarelli, B. *Biochem.* **1997**, *36*, 7847.
(27) Tard, C. D.; Liu, X.; Kalbrahim, S.; Bruschi, M.; Gioia, L. D.; Davies, S. C.; Yang, X.; Wang, L.-S.; Sawers, G.; Pickett, C. J. *Nature* **2005**, *433*, 610.

10.1021/ic0484699 CCC: $30.25
Published on Web 06/17/2005

On the basis of these calculations, the most probable pathway of the concerted proton transfer (PT) and electron transfer (ET) in the H_2 formation/cleavage reactions at $[FeFe]_H$ was suggested and rationalized.[35] Our mechanism stressed that the proximal iron Fe_p site is the activation center and that the hydride H^- bridging to the two iron atoms, Fe_p and Fe_d (distal iron), takes a central position in the proposed H_2 formation/cleavage mechanism. In the present work, we significantly expanded the previous models and performed large-scale DFT computations on the whole H cluster ([6Fe-6S] = $[4Fe\text{-}4S]_H + [FeFe]_H$) by including the important $[4Fe\text{-}4S]_H$ subcluster which acts as an electron reservoir.[10] The electron transfer between $[Fe_4S_4]_H^{2+}$ and $[FeFe]_H$ has been regarded as the driving force for dihydrogen bond formation and cleavage. Simplified models,[35] where the $[Fe_4S_4]_H^{2+}$ subcluster is not explicitly considered, were also employed whenever the subcluster is not actively involved in the reaction steps and acts as a spectator. In particular, we focused our investigation on the H−H bond formation and cleavage processes on Fe_p and identified a new intermediate state containing an $Fe_p\cdots H\cdots CN$ two-electron three-center (2e-3c) bond which occurs at the initial stage for the H−H bond formation and final stage for the H−H bond cleavage.

Computational Details

Calculations were performed using the DFT program Dmol[3] from the Cerius[2] software package.[36] Geometries of the various models were optimized by unrestricted spin-polarized (or different orbital for different spin, DODS) local DFT methods with the Perdew−Wang (1992) functional.[37] For the basis sets, we adopted the double numerical basis set containing a *p*-polarization for H and *d*-polarization for all other atoms (abbreviated as DNP). The DNP basis sets are given numerically as cubic spline functions, and their quality and size are comparable to the standard Gaussian 6-31G-(d,p) split-valence double-ζ plus polarization basis set. The numerical basis set, DNP, is the exact solution to the Kohn−Sham equations for atoms. By means of the potential energy surface (PES) scan, we searched the intermediate states with one imaginary frequency in the calculation of the second derivatives for the single-variable models of proton transfer from one site to the other. Here, the intermediate state is defined as the structure with the highest energy between two optimal energy-minimum structures on a PES scan and may be better described as an approximate (or quasi) transition state (TS). Simultaneously, searches for a multivariable transition state were conducted progressively using the LST/QST method[38] in the Materials Studio software package. [36]

Results and Discussion

Optimal Structures at Various Redox and Charge States. Because an iron atom with an oxidation state of 0, +1, +2, or +3 favors a high-spin state with its 3d shell partially occupied, there are significant spin polarization and coupling effects in many iron−sulfur protein enzymes.[39] As a result, ideally these systems should be described by a linear combination of various DODS wave functions (or states). Because the Dmol[3] program cannot deal with multiwave functions, the [4Fe-4S] cluster is mainly imposed as a spectator during the H_2 formation and cleavage processes. Consequently, we assume that the spin-coupled effect within the [4Fe-4S] cluster on the relative energy calculations of the H_2 cleavage may be insignificant, and in the following discussion, we only consider the low-spin state of the H cluster.

We started by considering four $[H\ cluster]_t$ models consisting of the $[FeFe]_H$ and $[4Fe\text{-}4S]_t$ moieties, where $[FeFe]_H$ ($[FeFe]_H = (CH_3S)(2CO)(CN)Fe_p(2H)(\mu\text{-}SRS)Fe_d(CO)(CN)$) contains two active hydrogen species ($H^+ + H^-$ or activated H_2) and the type label, t (t = a, b, c, d), denotes the extent of the simplification of the [4Fe-4S] subcluster (i.e., $[4Fe\text{-}4S]_a = Fe\text{-}[3(CH_3S{-}Fe)(3H)\text{-}4S]$, $[4Fe\text{-}4S]_b = Fe\text{-}[3(CH_3S{-}Fe)(2H)\text{-}4S]$, $[4Fe\text{-}4S]_c$ = H, and $[4Fe\text{-}4S]_d$ = null). The symbol $\mathbf{x}_t[y]_z$ is thus used to represent a model to make the following discussion concise and straightforward, where the serial number **x** distinguishes the structure of $[FeFe]_H$, y is the total charge, and z represents the redox state (i.e., z = ox is an oxidized state, $[Fe^{II}Fe^{II}]$, z = s is an EPR active semireduced state, $[Fe^{II}Fe^{I}]$ ($s = 1/2$), and z = red is a reduced state, $[Fe^{I}Fe^{I}]$). Both experimental and computational studies have suggested a catalytic cycle as follows: $Fe^{II}Fe^{II} \leftrightarrow Fe^{II}Fe^{I} \leftrightarrow Fe^{I}Fe^{I}$.[13,14,19,20] For simplicity and generality, we can further use the notation **x** to define a structure and the symbol $\mathbf{x}_z$ (e.g., $\mathbf{1}_{ox}$ or $\mathbf{1}_s$) to refer to a structure at an assigned redox state.

Our previous investigation with the simplified model $[H\ cluster]_c$ has confirmed the significance of the hydride bridging the Fe_p and Fe_d sites in the hydrogen generation and consumption by Fe-only H_2ases.[35] As our interest lies in the H−H bond formation and cleavage processes on Fe_p, we optimized four key models ($\mathbf{1}_a[1]_{ox}$, $\mathbf{1}_b[0]_{ox}$, $\mathbf{1}_c[0]_{ox}$, and $\mathbf{1}_d[-1]_{ox}$) as shown in Figure 1. Among these four models, $\mathbf{1}_a[1]_{ox}$ and $\mathbf{1}_b[0]_{ox}$ fall into the category of complete H cluster models, and they are correlated as $\mathbf{1}_a[1]_{ox} = \mathbf{1}_b[0]_{ox} + H^+$. The other two models, $\mathbf{1}_c[0]_{ox}$ and $\mathbf{1}_d[-1]_{ox}$, are simplified models, and $\mathbf{1}_c[1]_{ox} = \mathbf{1}_d[0]_{ox} + H^+$. These four models ($\mathbf{1}_a[1]_{ox}$, $\mathbf{1}_b[0]_{ox}$, $\mathbf{1}_c[0]_{ox}$ and $\mathbf{1}_d[-1]_{ox}$) can be uniformly denoted as $\mathbf{1}_{ox}$. The addition of one electron to $\mathbf{1}_{ox}$ results in

(28) Gloaguen, F.; Lawrence, J. D.; Rauchfuss, T. B. *J. Am. Chem. Soc.* **2001**, *123*, 9476.
(29) Gloaguen, F.; Lawrence, J. D.; Rauchfuss, T. B.; Benard, M.; Rohmer, M.-M. *Inorg. Chem.* **2002**, *41*, 6573.
(30) Zhao, X.; Georgakaki, I. P.; Miller, M. L.; Mejia-Rodriguez, R.; Chiang, C. Y.; Darcensbourg, M. Y. *Inorg. Chem.* **2002**, *41*, 3917.
(31) Zhao, X.; Chiang, C.-Y.; Miller, M. L.; Rampersad, M. V.; Darensbourg, M. Y. *J. Am. Chem. Soc.* **2003**, *125*, 518.
(32) Zhao, X.; Georgakaki, I. P.; Miller, M. L.; Yarbrough, J. C.; Darcensbourg, M. Y. *J. Am. Chem. Soc.* **2001**, *123*, 9710.
(33) Nehring, J. L.; Heinekey, D. M. *Inorg. Chem.* **2003**, *42*, 4288.
(34) Fiedler, A. T.; Brunold, T. C. *Inorg. Chem.* **2005**, *44*, 1794.
(35) Zhou, T.; Mo, Y.; Liu, A.; Zhou, Z.; Tsai, K. *Inorg. Chem.* **2004**, *43*, 923.
(36) (a) Delley, B. *J. Chem. Phys.* **1990**, *92*, 508. (b) Delley, B. *J. Chem. Phys.* **1991**, *94*, 7245. (c) Delley, B. *J. Chem. Phys.* **2000**, *113*, 7756. (d) Delley, B. In *Density Functional Theory: A Tool for Chemistry*; Seminario, J. M., Politzer, P., Eds.; Elsevier: Amsterdam, The Netherlands, 1995.
(37) Perdew, J. P.; Chevary, J. A.; Vosko, S. H.; Jackson, K. A.; Pederson, M. R.; Fiolhais, C. *Phys. Rev. B* **1992**, *46*, 6671.
(38) (a) Halgren, T. A.; Lipscomb, W. N. *Chem. Phys. Lett.* **1977**, *49*, 225. (b) Ayala, P. Y.; Schlegel, H. B. *J. Chem. Phys.* **1997**, *107*, 375.
(39) (a) Noodleman, L.; Lovell, T.; Han, W.-G.; Li, J.; Himo, F. *Chem. Rev.* **2004**, *104*, 459. (b) Lovell, T.; Himo, F.; Han, W.-G.; Noodleman, L. *Coord. Chem. Rev.* **2003**, *238*, 211. (c) Noodleman, L.; Peng, C. Y.; Case, D. A.; Mouesa, J.-M. *Coord. Chem. Rev.* **1995**, *144*, 199.

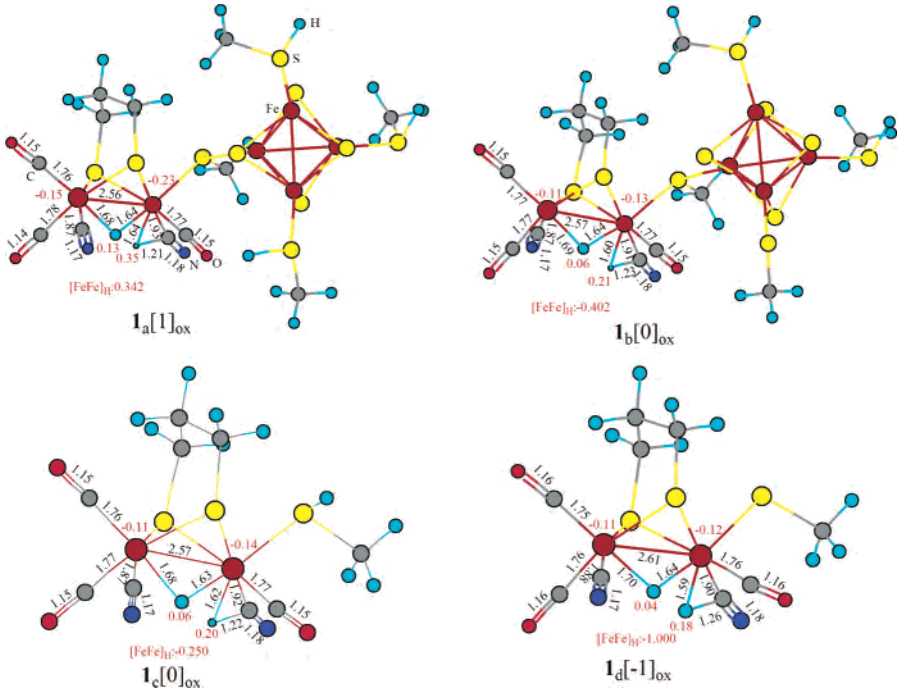

Figure 1. Four key models ($\mathbf{1}_a[1]_{ox}$, $\mathbf{1}_b[0]_{ox}$, $\mathbf{1}_c[0]_{ox}$, and $\mathbf{1}_d[-1]_{ox}$) with optimal structural parameters (in black) and Mulliken charges (in red, also listed is the total charge for the $[FeFe]_H$ moiety). The atoms are symbolized with colors (cyan for H, gray for C, red for O, blue for N, yellow for S, and brown for Fe).

a semireduced state, $\mathbf{1}_s$, which also has four models, $\mathbf{1}_a[0]_s$, $\mathbf{1}_b[-1]_s$, $\mathbf{1}_c[-1]_s$, and $\mathbf{1}_d[-2]_s$, and all eight models ($\mathbf{1}_a[1]_{ox}$, $\mathbf{1}_b[0]_{ox}$, $\mathbf{1}_c[0]_{ox}$, $\mathbf{1}_d[-1]_{ox}$, $\mathbf{1}_a[0]_s$, $\mathbf{1}_b[-1]_s$, $\mathbf{1}_c[-1]_s$, and $\mathbf{1}_d[-2]_s$) are collectively referred to as structure **1**. This class of structures shows energy-minimum states that were not previously determined. The unique characteristic for structure **1** is that there is one hydride bridging iron ions Fe_p and Fe_d and one proton participating in an $Fe_p\cdots H\cdots CN$ two-electron three-center bond. This seems to be in accordance with Bruschi's note[40] which states that the release of HCN from the optimized transition state in the proton transfer from the μ-SRS site to the Fe_p site can often be observed. Starting from structure **1**, we attempted to take the H−H distance as the reaction coordinate and derive energy profiles to find the energy-minimal structures, **2**, containing an $Fe_p\cdots\eta^2-H_2$ bond. However, we found that only for models $\mathbf{1}_b[-1]_s$, $\mathbf{1}_c[-1]_s$, $\mathbf{1}_d[-1]_{ox}$, and $\mathbf{1}_d[-2]_s$, can both the transition and product states on the energy profiles be successfully located. For models $\mathbf{1}_a[1]_{ox}$, $\mathbf{1}_a[0]_s$, $\mathbf{1}_b[0]_{ox}$, and $\mathbf{1}_c[0]_{ox}$, the molecular energy monotonically increases as the H−H bond distance decreases in the PES scan; thus, we were unable to locate structures $\mathbf{2}_a[1]_{ox}$, $\mathbf{2}_a[0]_s$, $\mathbf{2}_b[0]_{ox}$, and $\mathbf{2}_c[0]_{ox}$ because the optimizations uniformly converged to structure **1** (i.e., $\mathbf{1}_a[1]_{ox}$, $\mathbf{1}_a[0]_s$, $\mathbf{1}_b[0]_{ox}$, and $\mathbf{1}_c[0]_{ox}$). Model $\mathbf{3}_{ox}$ comes from a proton transfer from the $Fe_p\cdots H\cdots CN$ site in $\mathbf{1}_{ox}$ to the Cys-S site. The hopping of this proton in either $\mathbf{1}_{ox}$ or $\mathbf{3}_{ox}$ leads to structure $\mathbf{4}_{ox}$, in which the proton is bonded to μ-SRS. Obviously, for type c where $[4Fe\text{-}4S]_c = H$, we cannot put two H atoms on CH_3-S, with one H representing the [4Fe-4S] cluster and one H representing the transferable proton. Therefore, it is impossible to locate the structure **3** for type c. The transition state from $\mathbf{1}_s$ to $\mathbf{2}_s$ is defined as structure $\mathbf{5}_s$, and structure $\mathbf{6}_{ox}$ is the transition state from $\mathbf{3}_{ox}$ to $\mathbf{4}_{ox}$. For the process $\mathbf{1}_{ox} \leftrightarrows \mathbf{4}_{ox}$, the transition state is $\mathbf{7}_{ox}$. However, in the optimal geometry of model $\mathbf{6}_b[0]_{ox}$, as shown in Figure 2, the migrating proton is simultaneously in close contact with Fe_p (1.67 Å), Cys-S (1.89 Å), and μ-SRS (1.57 Å). Thus, $\mathbf{6}_b[0]_{ox}$ seems to be not only the transition state for the $\mathbf{3}_b[0]_{ox} \leftrightarrows \mathbf{4}_b[0]_{ox}$ process, but also very close to the transition states for the other two processes, $\mathbf{3}_b[0]_{ox} \leftrightarrows \mathbf{1}_b[0]_{ox}$ and $\mathbf{1}_b[0]_{ox} \leftrightarrows \mathbf{4}_b[0]_{ox}$. A reaction flowchart and the associated energy changes for the proton and electron transfers are presented in Figure 3.

To differentiate the models with the same structure, **x**, and different types, t, we computed the sum of Mulliken atom charges in the $[FeFe]_H$ part (Figures 1 and 2). We found that the CO, CN, Fe−Fe bond length, and, particularly, the C−H distances in the $Fe_p\cdots H\cdots CN$ two-electron three-center bond of structure **1** shown in Figures 1 and 2 and the reaction energies in Figure 3 from structures **1** to **2** are closely related to the total Mulliken atomic charges in the $[FeFe]_H$ part and the acid−base characters of the models, as shown in Figure 4. The [4Fe-4S] part imposes its role of "spectator" via electrostatic interactions with $[FeFe]_H$. Structure $\mathbf{1}_a[1]_{ox}$ with a positive Mulliken charge (0.342 e) in the $[FeFe]_H$ part is assumed to be a weak acid model and favorable for $Fe_p\cdots H\cdots CN$ bond formation on the basis of the structural data in Figure 1. In fact, we found that the higher the positive charge on $[FeFe]_H$, the stronger the $Fe_p\cdots H\cdots CN$ bond. Models of type a are not active for H−H bond formation in the Fe_P site, and thus, $\mathbf{1}_a[1]_{ox}$ could be taken as a model for the isolated oxidized state. In contrast, weak basic models of types b and c favor the H−H bond formation and cleavage

(40) (a) Bruschi, M.; Fantucci, P.; Gioia, L. *Inorg. Chem.* **2002**, *41*, 1421. (b) Bruschi, M.; Fantucci, P.; Gioia, L. *Inorg. Chem.* **2003**, *42*, 4773. (c) Bruschi, M.; Fantucci, P.; Gioia, L. *Inorg. Chem.* **2004**, *43*, 3733.

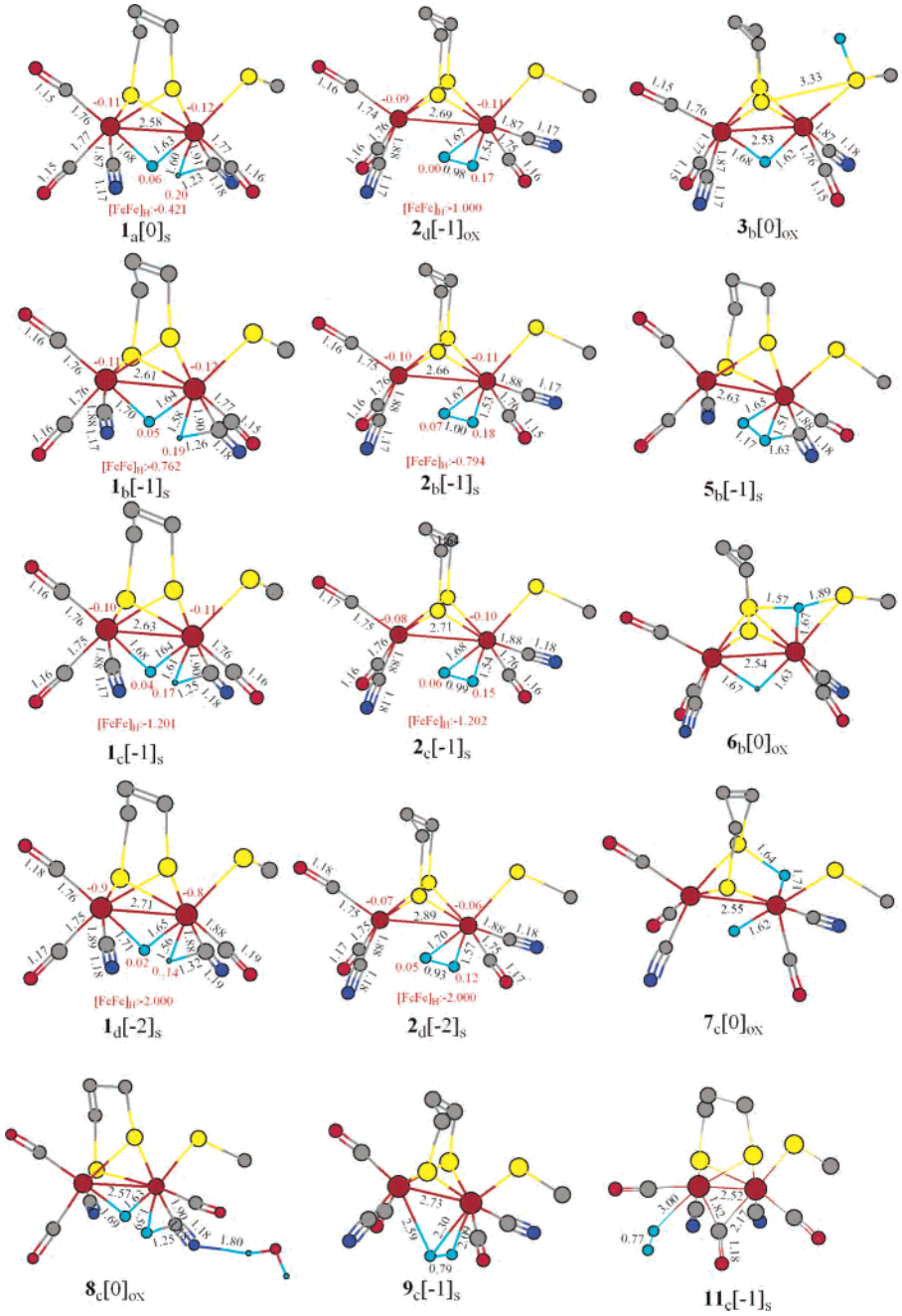

Figure 2. Optimal geometries and Mulliken charges of various important models. For simplicity, the $[4Fe\text{-}4S]_t$ part and hydrogen atoms in PDT and $-CH_3$ are not shown.

reactions, and models of type d are stronger bases than those of type c; therefore, they are more favorable for the formation of the H−H bond. Particularly, model $\mathbf{1}_b[-1]_s$, a weak base, is active for both the H−H bond formation and cleavage processes with very low activation barriers. On the basis of these results, discussed above, we conclude that the models of type b are the most rational models with which to study the reversible hydrogen oxidation.

For the three identical reactions $\mathbf{3}_a[1]_{ox} - 1.4$ kcal/mol $\leftrightarrows$ $\mathbf{4}_a[1]_{ox}$, $\mathbf{3}_b[0]_{ox} + 2.0$ kcal/mol $\leftrightarrows$ $\mathbf{4}_b[0]_{ox}$ and $\mathbf{3}_d[-1]_{ox} + 15.3$ kcal/mol $\leftrightarrows$ $\mathbf{4}_d[-1]_{ox}$, we found a remarkable discrepancy among their reaction energies, which once again confirms that the simplified models cannot rationally predict the proton transfer from Cys-S to other parts of the $[FeFe]_H$ cluster and highlights the importance of the explicit consideration of the [4Fe-4S] part. In the optimal structures of $\mathbf{1}_d[-2]_s$ and $\mathbf{2}_d[-2]_s$, the distances of the Fe−Fe, CO, and CN bonds are unanimously much larger than the experimental values (Figure 2); this suggests that the simplified models of type d with large negative charges are unreliable. However, by comparing the $\mathbf{1}_b[0]_{ox} + 3.2$ kcal/mol $\leftrightarrows$ $\mathbf{4}_b[0]_{ox}$, $\mathbf{1}_b[-1]_s +$ 0.4 kcal/mol $\leftrightarrows$ $\mathbf{2}_b[-1]_s$ and $\mathbf{1}_c[0]_{ox} + 2.4$ kcal/mol $\leftrightarrows$ $\mathbf{4}_c[0]_{ox}$, $\mathbf{1}_c[-1]_s - 0.4$ kcal/mol $\leftrightarrows$ $\mathbf{2}_c[-1]_s$ reactions, we found that their reaction energies (3.2 vs 2.4 kcal/mol and 0.4 vs. −0.4 kcal/mol) are very close. In addition, model $\mathbf{1}_c[-1]_s$ is also a weak base, and the Mulliken charges of the same structures of b and c are similar (see Figures 1 and 2). As a result, simplified model structures of type c are also used in our

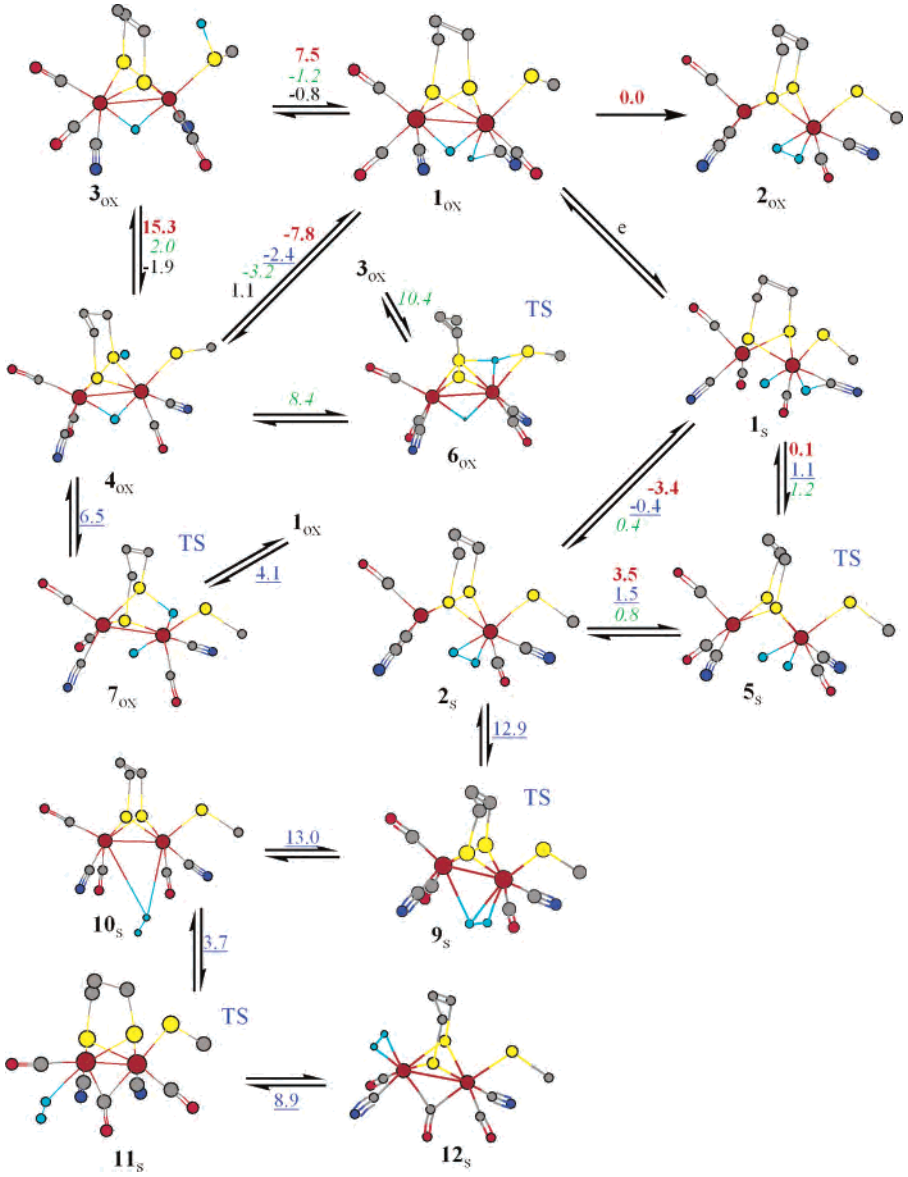

Figure 3. Proton transfer (PT) reaction flowchart where the $[4Fe\text{-}4S]_t$ part and hydrogen atoms in PDT and $-CH_3$ are not shown. $\mathbf{x}_z$ corresponds to a structure at the assigned redox state, and the data on the arrowheads are the reaction energies in kcal/mol (black plain text for model type a, green italic text for type b, blue underlined text for type c, and red bold text for type d).

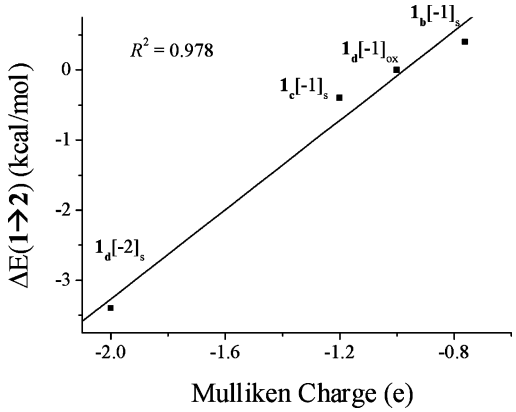

Figure 4. Correlation between the reaction energies (kcal/mol) from **1** to **2** and the overall Mulliken charges for the $[FeFe]_H$ part.

subsequent calculations and discussion when the $[Fe_4S_4]_H^{2+}$ subcluster is not directly involved in the reactions.

Because our computations are conducted in the gas phase, one question related to the new intermediate state, **1**, is whether the $Fe_p\cdots H\cdots CN$ two-electron three-center bond could exist in a protein environment and aqueous solution, as the surrounding amino acid residues or water molecules could form hydrogen bonds with the CN^- ligands in the $[FeFe]_H$ which would subsequently disfavor the two-electron three-center bond. To confirm the existence of such an $Fe_p\cdots H\cdots CN$ bond, we put water molecules around CN^-, fixed the $N\cdots H$ distance at 1.8 Å, and optimized the resulting structure, $\mathbf{8}_c[0]_{ox} = \mathbf{1}_c[0]_{ox} + H_2O$. Figure 2 shows the optimal geometry of $\mathbf{8}_c[0]_{ox}$. We found that the $Fe_p\cdots H\cdots CN$ bond in model $\mathbf{8}_c[0]_{ox}$ is only slightly weaker than that in $\mathbf{1}_c[0]_{ox}$. Thus, we surmise that the possible hydrogen bond between the CN^- ligand and the surroundings imposes a negligible effect on the unique $Fe_p\cdots H\cdots CN$ bond in intermediate structure **1**.

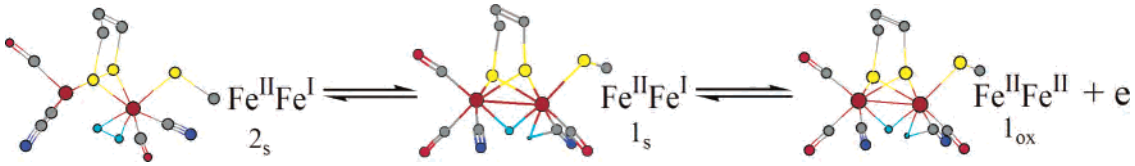

H−H Bond Formation and Cleavage on $[FeFe]_H$. The conversion between $\mathbf{1}_s$ and $\mathbf{2}_s$ requires very little energy ($\mathbf{1}_b[-1]_s$ + 0.4 kcal/mol ⇆ $\mathbf{2}_b[-1]_s$ or $\mathbf{1}_c[-1]_s$ − 0.4 kcal/mol ⇆ $\mathbf{2}_c[-1]_s$) with a very low activation barrier ($\mathbf{1}_b[-1]_s$ + 1.2 kcal/mol ⇆ $\mathbf{5}_b[-1]_s$ (TS) and $\mathbf{5}_b[-1]_s$ − 0.8 kcal/mol ⇆ $\mathbf{2}_b[-1]_s$ or $\mathbf{1}_c[-1]_s$ + 1.1 kcal/mol ⇆ $\mathbf{5}_c[-1]_s$ (TS) and $\mathbf{5}_c[-1]_s$ − 1.5 kcal/mol ⇆ $\mathbf{2}_c[-1]_s$) as shown in Figure 3. These data are in agreement with the experimental findings and confirm that Fe−H_2ases can catalyze both the H−H formation and cleavage reactions efficiently. Because the H−H formation and cleavage directions are closely related to the total charge in the $[FeFe]_H$ part, as shown in Figure 4, the ET between $[Fe_4S_4]_H^{2+}$ and $[FeFe]_H$ is regarded as the driving force for the generation and consumption of hydrogen. The process from **2** to **1** corresponds to the splitting of the H−H bond as shown above.

Hall and co-workers[19,20] considered that a hydride is bound to the terminal Fe_d in $[FeFe]_H$. Spectroscopically, such an intermediate remains undetected in enzyme systems, and no synthetic diiron thiolate models with terminally bound hydrides have ever been characterized.[4] In contrast, model complexes n−H^+ = [Fe^{II}(μ-H)Fe^{II}] containing a bridge hydride[28−33] can be easily produced via the protonation of n = [$Fe^{I}Fe^{I}$] (n + H^+ ⇆ n−H^+), and subsequently, H_2 is generated through the reaction n−H^+ + 2e + H^+ ⇆ n + H_2.[28,29] The position of the bridging hydride in n−H^+ has been located by NMR spectra.[29] Thus, the probable existence of the structures of **2** and **3** proposed in this work could be experimentally verified. Zhao et al. pointed out that the formation of H_2 must be preceded by a reduction to the Fe^{II}-Fe^{I} redox state;[30] our calculations on models of types b and c, shown in Figure 3, supported this assumption. As structure **1** is the key to the present mechanism, experimental verifications of the existence of the Fe_p···H···CN two-electron three-center bond in Fe−H_2ases or related model complexes are vital for endorsing our mechanism. From the structural point of view, the Fe_P−CN bond in **1** is about 0.02−0.07 Å longer than those in models **2** and **3**, while the Fe_PC−N bond changes negligibly on the basis of the optimized geometries of models of types a and b, as compiled in Table 1; thus, the change of the Fe_P−CN bond can be an indicator for the existence of the two-electron three-center bond.

In addition, the $\mathbf{2}_s$ ⇆ $\mathbf{9}_s$ (TS) ⇆ $\mathbf{10}_s$ and $\mathbf{10}_s$ ⇆ $\mathbf{11}_s$ (TS) ⇆ $\mathbf{12}_s$ processes have relatively low reaction energies, from our previous work,[35] and in $\mathbf{10}_s$, the dihydrogen can practically be seen as a free H_2 molecule. The multivariable transition states $\mathbf{9}_c[-1]_s$ and $\mathbf{11}_c[-1]_s$ were solved using the LST/QST/CG method[38] as illustrated in Figure 5. Therefore, the three states ($\mathbf{2}_s$, $\mathbf{10}_s$, and $\mathbf{12}_s$) could easily interchange from one to another with very low activation barriers. The $\mathbf{10}_s$ ⇆ $\mathbf{12}_s$ process refers to the hopping of CO from an Fe_d terminal site to a bridging site[7] (Fe_p···(η^{2-}-H_2)···Fe_d + Fe_d−CO ⇆ Fe_p···(CO)···Fe_d + Fe_d−(η^2-H_2)). Finally, H_2 evolves from Fe_d.[3,41]

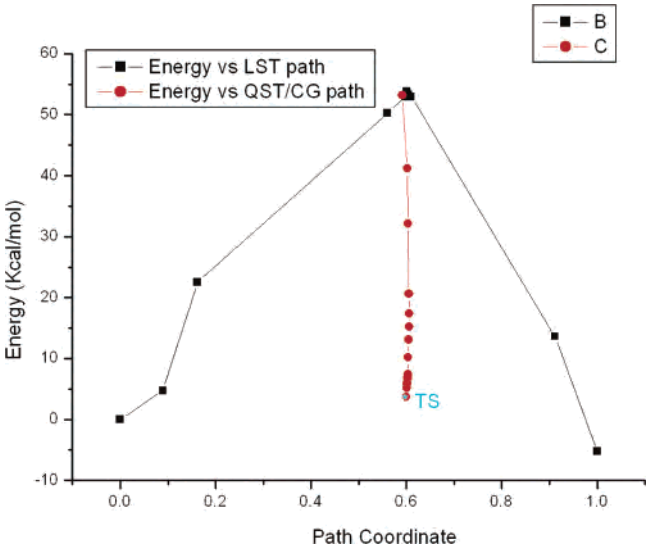

Figure 5. Search of transition state $\mathbf{11}_c[-1]_s$ from $\mathbf{10}_c[-1]_s$ to $\mathbf{12}_c[-1]_s$ by means of the LST/QST/CG strategy.

Table 1. Optimal Fe_P−CN and Fe_PC−N Bond Lengths in Structures **1**, **2**, and **3** (Å)

	$\mathbf{1}_a[1]_{ox}$	$\mathbf{3}_a[1]_{ox}$	$\mathbf{1}_b[0]_{ox}$	$\mathbf{3}_b[0]_{ox}$	$\mathbf{1}_a[0]_s$	$\mathbf{1}_b[-1]_s$	$\mathbf{2}_b[-1]_s$
Fe_P−CN	1.926	1.862	1.912	1.865	1.912	1.904	1.876
Fe_PC−N	1.176	1.174	1.177	1.175	1.178	1.179	1.173

Conclusion

On the basis of the extended model studies of Fe-only hydrogenases with density functional theory, we identified a new intermediate state with an Fe_p···H···CN two-electron three-center bond. This intermediate state is assumed to play an important role in the proton and electron transfers and, subsequently, in the reversible hydrogen oxidation in hydrogenases, which are essential for the elucidation of the potent catalytic power of this type of enzymes to generate and consume hydrogen.

Acknowledgment. This work has been supported by State Key Laboratory for Physical Chemistry of Solid States at Xiamen University. Partial support from Western Michigan University is gratefully acknowledged (Y.M.). We thank Dr Kai Tan and Dr Ze-Xing Cao for their help with the calculations of the transition state using the Materials Studio software package.

Supporting Information Available: Cartesian coordinates for the optimal geometries of various models. This material is available free of charge via the Internet at http://pubs.acs.org.

IC0484699

(41) Igarashi, R. Y.; Laryukhin, M.; Dos Santos, P. C.; Lee, H.-I.; Dean, D. R.; Seefeldt, L. C.; Hoffman, B. M. *J. Am. Chem. Soc.* **2005**, *127*, 6231.